AL/EQ-TR-1993-0306

DENSE-GAS DISPERSION IN COMPLEX TERRAIN

Donald L. Ermak

Lawrence Livermore National Laboratory
P.O. Box 808
Livermore, CA 94550

Contract No. F08635-92-C-0056

May 1993

ENVIRONICS DIRECTORATE
ARMSTRONG LABORATORY

■ **Air Force Materiel Command** ■ **United States Air Force** ■ **Tyndall Air Force Base, FL 32403-5323**

REPORT DOCUMENTATION PAGE

Form Approved
OMB No. 0704-0188

PLEASE DO NOT RETURN YOUR FORM TO THE ABOVE ADDRESS.

1. REPORT DATE *(DD-MM-YYYY)*	2. REPORT TYPE	3. DATES COVERED *(From - To)*
01-MAY-1993	Technical Report	01-OCT-1990 -- 31-DEC-1991

4. TITLE AND SUBTITLE

Dense-Gas Dispersion in Complex Terrain

5a. CONTRACT NUMBER

F08635-92-C-0056

5b. GRANT NUMBER

5c. PROGRAM ELEMENT NUMBER

6. AUTHOR(S)

Ermak, Donald L.

5d. PROJECT NUMBER

5e. TASK NUMBER

5f. WORK UNIT NUMBER

21032016

7. PERFORMING ORGANIZATION NAME(S) AND ADDRESS(ES)

Lawrence Livermore National Laboratory
P.O. Box 808
Livermore, CA 94550

8. PERFORMING ORGANIZATION REPORT NUMBER

9. SPONSORING/MONITORING AGENCY NAME(S) AND ADDRESS(ES)

Environics Directorate
Air Force Engineering and Service Center
139 Barnes Drive, Suite 2
Tyndall Air Force Base, FL 32403-5323

10. SPONSOR/MONITOR'S ACRONYM(S)

AL/EQ

11. SPONSOR/MONITOR'S REPORT NUMBER(S)

AL/EQ-TR-1993-0306

12. DISTRIBUTION/AVAILABILITY STATEMENT

Distribution Statement A: Approved for public release; distribution unlimited.

13. SUPPLEMENTARY NOTES

14. ABSTRACT

A dense-gas version of the ADPIC Lagrangian particle, advection-diffusion model has been developed to simulate the atmospheric dispersion of denser-than-air releases over complex terrain. In developing the model, it was assumed that the dense-gas effects could be described in terms of the vertically-averaged thermodynamic properties and the local height of the cloud. The dense-gas effects were treated as a perturbation to the ambient thermodynamic properties (density and temperature), ground level heat flux, turbulence level (diffusivity), and windfield (gravity flow) within the local region of the dense-gas cloud. These perturbations were calculated from conservation of energy and conservation of momentum principles along with the ideal gas law equation of state for a mixture of gases. ADPIC, which is generally run in conjunction with a mass-conserving wind flow model to provide the advection field, contains all the dense-gas modifications within it. This feature provides the versatility of coupling the new dense-gas ADPIC with alternative wind flow models. The new dense-gas ADPIC has been used to simulate the atmospheric dispersion of ground-level, colder-than-ambient, denser-than-air releases and has compared favorably with the results of field-scale experiments.

15. SUBJECT TERMS

dense-gas dispersion, dispersing, dispersions, gases

16. SECURITY CLASSIFICATION OF:			17. LIMITATION OF ABSTRACT	18. NUMBER OF PAGES	19a. NAME OF RESPONSIBLE PERSON
a. REPORT	b. ABSTRACT	c. THIS PAGE			Michael Moss
U	U	U	UU	22	19b. TELEPHONE NUMBER *(Include area code)*

Reset

Standard Form 298 (Rev. 8/98)
Prescribed by ANSI Std. Z39.18

UCRL-JC-
PREPRINT

Final Report:

Dense-Gas Dispersion In Complex Terrain

Donald L. Ermak

This paper was prepared for submittal to the
U.S. Air Force Engineering and Service Center
Tyndall Air Force Base
(MIPR N90-29)

May 1993

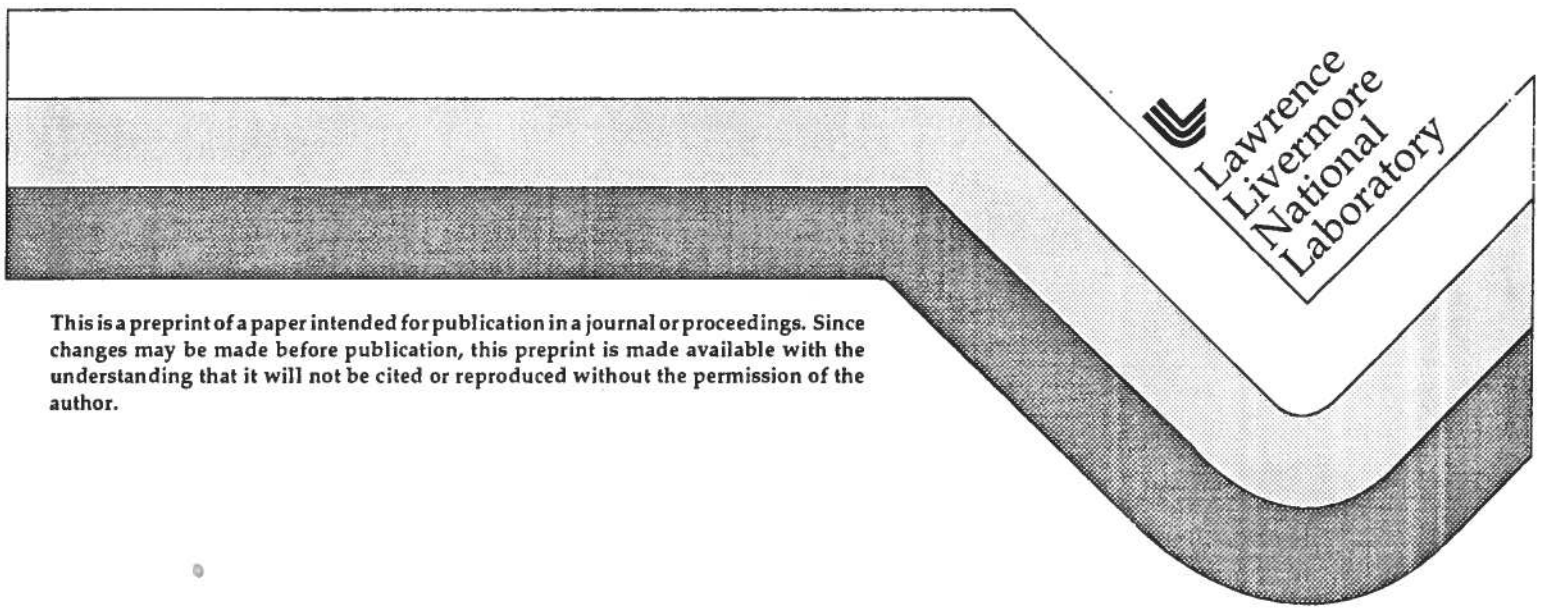

FINAL REPORT:

DENSE-GAS DISPERSION IN COMPLEX TERRAIN

D.L. Ermak
Lawrence Livermore National Laboratory
Livermore, California 94550

ABSTRACT

A dense-gas version of the ADPIC Lagrangian particle, advection-diffusion model has been developed to simulate the atmospheric dispersion of denser-than-air releases over complex terrain. In developing the model, it was assumed that the dense-gas effects could be described in terms of the vertically-averaged thermodynamic properties and the local height of the cloud. The dense-gas effects were treated as a perturbation to the ambient thermodynamic properties (density and temperature), ground level heat flux, turbulence level (diffusivity), and windfield (gravity flow) within the local region of the dense-gas cloud. These perturbations were calculated from conservation of energy and conservation of momentum principles along with the ideal gas law equation of state for a mixture of gases. ADPIC, which is generally run in conjunction with a mass-conserving wind flow model to provide the advection field, contains all the dense-gas modifications within it. This feature provides the versatility of coupling the new dense-gas ADPIC with alternative wind flow models. The new dense-gas ADPIC has been used to simulate the atmospheric dispersion of ground-level, colder-than-ambient, denser-than-air releases and has compared favorably with the results of field-scale experiments.

INTRODUCTION

A popular approach to simulating the atmospheric dispersion of trace-gas releases under realistic conditions of terrain and varying winds is to use a Lagrangian particle, advection-diffusion model such as ADPIC[1, 2]. These codes are well suited to operational uses for emergency response and accident preparedness purposes[3] due to their robustness and relatively high computational speed on present day computers. While advection-diffusion models have been extensively used and validated against numerous field tests of trace gas releases, they do not contain the necessary physics to simulate the atmospheric dispersion of denser-than-air-releases. To overcome this limitation, we have developed a dense-gas version of ADPIC.

The atmospheric dispersion of denser-than-air gases requires a somewhat different approach to modeling than the more conventional one used for the dispersion of trace gases[4, 5]. In a trace-gas release, the quantity of material released to the atmosphere is too small to have any significant effect upon the atmospheric flow into which it is mixing. Consequently, trace-gas dispersion is controlled solely by the advective and diffusive properties of the ambient atmosphere. On the other hand, a dense-gas release behaves more like an independent, continuous cloud whose physical properties (density, temperature, turbulence level) are significantly different than those of the ambient atmosphere. Under these conditions, the dispersion of a dense-gas cloud is controlled as much, if not more, by these in-cloud properties as by the conditions existing in the ambient atmosphere.

Several major effects are observed in the dispersion of dense-gas clouds released at ground level that are not observed in the dispersion of trace emissions. One is a reduction of turbulent mixing in the vertical direction of the vapor cloud with the ambient atmosphere due to stable density stratification of the cloud relative to the above-lying ambient air. Another is the generation of gravity-spreading flow due to density gradients in the horizontal direction. These two effects result in a lower and significantly wider cloud than is observed when a trace or neutral density gas is released. In addition, dense-gas clouds tend to follow the downhill slope independent of the wind direction and can become "trapped" in valleys or low spots. And when the release is a cold, dense-gas (i.e., LNG), the ground surface heat flux into the cloud may also play a significant role in the dispersion of the cloud.

Dense-gas dispersion effects are most pronounced when the ambient wind speed is low and the atmospheric stability conditions are stable. As the cloud mixes with the surrounding ambient atmosphere, the cloud becomes more dilute, the in-cloud properties approach ambient levels, and

the above mentioned effects begin to play a less significant role. Eventually, after a considerable amount of dilution, the originally dense-gas cloud begins to disperse like a trace-gas cloud where dispersion is primarily controlled by the ambient wind speed and atmospheric stability.

In the development of the dense-gas version of ADPIC, we assumed that the dense-gas effects could be described by the vertically-averaged thermodynamic properties of the cloud and the local cloud height. This simplification has been successfully employed in one-dimensional dense-gas dispersion models[6] and basically assumes that the dense-gas cloud is relatively thin in comparison to its horizontal dimensions. We then treated the dense-gas effects as perturbations to the ambient conditions within the local region of the dense-gas cloud[7]. Submodels for the friction velocity, turbulent diffusivity, and ground heating rate were adapted from the SLAB[6] and FEM3[8] models, both of which have been tested and validated extensively by comparison with laboratory and field-scale dispersion tests[9–11].

In this report, we describe the dense-gas version of ADPIC, the results from simulations of two field-scale dense-gas dispersion experiments, and a calculation of a dense-gas flow up a ramp. The following section includes a mathematical description of the Lagrangian particle advection-diffusion model and the main dense-gas modifications to the model. This is followed by a description of the code structure with regard to the new modifications and then the results from the model simulations. The experiments being simulated involved the large-scale release of liquefied natural gas (LNG) onto a pond of water with the atmospheric dispersion occurring principally over land with nearly flat terrain. The ramp calculation involves the dispersion of an instantaneous sulfur dioxide (SO_2) release at the base of a ramp and demonstrates the ability of the model to simulate dispersion over variable terrain.

MODEL DESCRIPTION

LAGRANGIAN PARTICLE, ADVECTION-DIFFUSION MODEL

The ADPIC atmospheric dispersion model is based upon the single conservation of species principal. This principal is expressed by the advection-diffusion equation as

$$\frac{\partial C}{\partial t} + \nabla \cdot \left(\bar{U}_a \, C \right) = \nabla \cdot \left(K \, \nabla C \right) \tag{1}$$

where C is the concentration of the gas released into the atmosphere, $\bar{U}_a$ is the nondivergent $\left(\nabla \cdot \bar{U}_a = 0 \right)$ advection field (ambient wind velocity), and K is the ambient atmospheric turbulent diffusivity. The ambient advection field $\bar{U}_a$ is usually calculated in a separate, mass-conserving, wind flow model from a limited set of wind speed and direction observations. The turbulent diffusivity K is a function of the ambient atmospheric conditions and is calculated within the ADPIC code.

In the Lagrangian particle numerical integration technique used in ADPIC, the mass of the released gas is represented by marker particles. The dispersion of the released gas is simulated by the marker particle trajectories which are calculated from a displacement equation that is derived from the advection-diffusion equation. Consequently, the distribution of marker particles in time and space represents the concentration distribution of the released gas. In the ADPIC code, the concentration within a particular volume element is calculated by summing the total mass within the volume element as represented by the marker particles and then dividing this sum by the volume of the volume element.

The marker particle displacement equations used in ADPIC are stochastic in nature and include both deterministic and random terms. The form we use is adapted from Boughton, *et al.*[12] and is

$$\begin{aligned} X(t+\Delta t) &= X(t) + U_a \cdot \Delta t + R_x(\Delta t) \\ Y(t+\Delta t) &= Y(t) + V_a \cdot \Delta t + R_y(\Delta t) \\ Z(t+\Delta t) &= Z(t) + W_a \cdot \Delta t + v_o \cdot \Delta t + R_z(\Delta t) \end{aligned} \tag{2a}$$

where $U_a, V_a,$ and W_a are the three components of the ambient wind velocity and $R_x, R_y,$ and R_z are three independent Gaussian random displacements with the mean and mean square properties

(2b)

$$\langle R_x \rangle = 0, \ \langle R_x^2 \rangle = 2 \cdot K_x \cdot \Delta t$$
$$\langle R_y \rangle = 0, \ \langle R_y^2 \rangle = 2 \cdot K_y \cdot \Delta t$$
$$\langle R_z \rangle = 0, \ \langle R_z^2 \rangle = 2 \cdot K_o \cdot \Delta t + v_o^2 \cdot \Delta t^2, \text{ where}$$
$$K_o = K_z(Z_o), \ Z_o = Z(o),$$
$$v_o = \frac{\partial K_z(Z_o)}{\partial Z}, \text{ and}$$
$$\langle \ \rangle = \text{average value.}$$

In Eq. (2), the terms involving $\overline{U}_a$ are the advective displacement and those involving K are the diffusive displacement. The advective displacement is deterministic, while the diffusive displacement includes both deterministic and random terms. When the diffusivity is homogeneous, as is assumed here for the two horizontal directions, the diffusive displacement contains only random terms. However, when it is inhomogeneous, as is the case in the vertical direction, then there is an additional deterministic term involving the gradient of the diffusivity.

Calculating the marker particle trajectories using Eq. (2) and then calculating the concentration from the distribution of marker particles is equivalent to calculating the concentration by directly solving the advection-diffusion, partial differential equation as expressed in Eq. (1). A major advantage of the stochastic, Lagrangian particle method is that it does not require the use of a fixed grid to calculate the particle trajectories, while the numerical solution of a partial differential equation does. This advantage is especially important when simulating dense-gas dispersion since the low-lying nature of dense-gas clouds may preclude (from a practical standpoint) the accurate determination of the cloud height and vertical cloud structure, when required to use a fixed grid.

DENSE GAS EFFECTS AND MODIFICATIONS

Our treatment of dense-gas dispersion within the ADPIC advection-diffusion model framework requires modification of the ambient wind field $\overline{U}_a$ and the vertical diffusivity K_z, and inclusion of surface heating J_g of the cloud at the ground. The modifications to the wind

field and diffusivity within the local region of the dense-gas cloud are due, for the most part, to the higher density of the cloud relative to the ambient atmosphere, and they directly effect the advection and diffusion terms in Eq. (2) for the marker particle displacement. Surface heating of the cloud is coupled to these advection and diffusion effects since it warms the cloud and thereby lowers the cloud density. Surface heating also adds a term to the vertical displacement equation due the expansion of the cloud associated with the heat gain.

Vertical Averaging. The dense-gas modifications are calculated by using a two-dimensional extension of the one-dimensional SLAB[6] model approach. This approach is based on the assumption that the dense-gas cloud height is relatively low in comparison to its horizontal dimensions. Consequently, cloud behavior is assumed to be described by the layer-(height-) averaged cloud properties and the thickness (cloud height) of the layer.

Using density as an example, the vertically averaged cloud density is defined to be

$$\rho(x,y) = \frac{1}{h} \cdot \int_o^h dz \cdot \rho(x,y,z), \tag{3}$$

where $\rho = \rho(x,y)$ is density, $h = h(x,y)$ is the cloud height, and both ρ and h are functions of the two horizontal coordinates x and y. For a cloud at ground level, the cloud height h is defined in terms of the mean squared marker particle height such that

$$h^2 = 3 \cdot \overline{Z}^2. \tag{4}$$

For the purpose of calculating the dense gas modifications, a three-dimensional description of the dense gas cloud is obtained by assuming vertical profiles for the cloud properties. Using the above example of density,

$$\rho(x,y,z) = \rho(x,y) \cdot f(z), \tag{5}$$

where $f(z)$ is a convenient function of height such as a step, Gaussian, or other simple analytic function. (The three-dimensional concentration distribution is still determined from the marker particle locations; however, the concentration distribution is not required at each step of the numerical integration of the marker particle trajectories.) The vertically averaged cloud properties of primary importance are cloud height, density, and temperature. The various dense

gas modifications are all expressed in terms of these layer-averaged quantities and, when necessary, an assumed vertical profile.

Gravity Flow, Dense-Gas Diffusivity, and Ground Heating. The dense-gas modification to the advection field replaces the ambient wind field $\overline{U}_a$ with a new wind field $\overline{U}$ that includes the effects of gravity flow. Treating gravity flow as a perturbation to the ambient flow, the new wind field can be expressed as

$$\overline{U}(x,y,z) = \overline{U}_a(x,y,z) + \overline{U}_g(x,y) \cdot g_i(z) \tag{6}$$

where

$\overline{U}_a(x,y,z)$ = ambient wind field

$\overline{U}_g(x,y)$ = vertically averaged gravity flow field perturbation

$g_i(z)$ = velocity profile function where $i = h$ (horizontal) or $i = v$ (vertical).

The vertically averaged, horizontal components of the gravity flow field are obtained by equating the gravitational force terms (using the hydrostatic approximation) to the dissipative terms due to air entrainment and surface friction, yielding

$$\begin{aligned} \rho\omega_e U_g &= -\frac{d}{dx}\left[0.5g(\rho-\rho_a)h^2\right] - g(\rho-\rho_a)h\frac{dH}{dx} - \rho u_f U_g \\ \rho\omega_e V_g &= -\frac{d}{dy}\left[0.5g(\rho-\rho_a)h^2\right] - g(\rho-\rho_a)h\frac{dH}{dy} - \rho u_f V_g \end{aligned} \tag{7}$$

where ω_e = entrainment rate

g = acceleration of gravity

h = cloud height above terrain

H = terrain height

u_f = surface friction coefficient

The entrainment rate ω_e is the rate at which air mixes into the dense-gas cloud from above and is taken to be proportional to the vertical diffusivity $K_z(h)$ divided by the cloud height h. The vertical component of the gravity flow field is obtained from the nondivergence condition $\left(\nabla \cdot \overline{U} = o\right)$ and is

$$W_g \cdot g_v(z) = -\left(\frac{\partial U_g}{\partial x} + \frac{\partial V_g}{\partial y}\right) \cdot \int_o^z dz\, g_h(z) \tag{8}$$

Equation (8) defines the relationship between the horizontal velocity profile function $g_h(z)$ and the vertical velocity profile function $g_v(z)$. By choosing $g_h(z)$ judiciously, both $g_h(z)$ and $g_v(z)$ can be analytical functions.

The new vertical diffusivity is adapted from the *K*-theory diffusivity used in the FEM3[8] three-dimensional, conservation equation model for dense gas dispersion. For a cloud within the surface layer, the new diffusivity is

$$\begin{aligned} K_z &= \frac{k \cdot u_* \cdot z}{\Phi} \\ \text{where } \Phi &= 1 + 5 \cdot z / L \\ L^{-1} &= L_a^{-1} + 2 \cdot g \cdot k^2 \cdot (\rho - \rho_a) / (\rho \cdot u_*^2) \\ u_* &= \text{friction velocity.} \end{aligned} \tag{9}$$

This form of the diffusivity is obtained from the well known similarity arguments of Monin and Obukhov and is such that it approaches the ambient diffusivity as the cloud density approaches the ambient level.

To account for ground heating of a cold, dense-gas cloud, we use a simple heat-transfer model

$$J_g = \rho \cdot C_p \cdot V_h \cdot (T_g - T) \tag{10}$$

where J_g is the ground flux of heat into the cloud, V_h is a representative energy-transfer velocity, T_g is the ground temperature, and ρ, C_p and T are the local layer-averaged cloud density, specific heat, and temperature, respectively. In the simulations of a cold, dense-gas release, we have found it adequate to replace the ground temperature T_g with the ambient air temperature T_a.

Thermodynamic Properties. The vertically averaged cloud density is obtained from the ideal gas law and is calculated from the location and mass of the marker particles. For a two species system of released gas and air at constant pressure, the ideal gas law can be expressed as

$$\rho = \frac{\rho_a T_a}{T} + \frac{(M_s - M_a)}{M_s} \cdot \rho_e \tag{11}$$

where ρ, ρ_e, and T are the vertically averaged cloud density, released gas density, and cloud temperature, ρ_a is the ambient air density at the ambient temperature T_a, and M_a and M_S are the molecular weights of air and the released gas.

The vertically averaged released gas density is defined to be

$$\rho_e = \left(\sum_n \omega_n \cdot q_n \right) / (A \cdot h) \tag{12}$$

where $q_n = q$ is the constant mass associated with each marker particle, ω_n is a position dependent weighting factor, h is the cloud height, and the sum is over all marker particles within the rectangular column of horizontal area A. The weighting factor is calculated by treating each marker particles as if it were a "square" with an area equal to the grid cell area and centered at the location of the marker particle. This weighted-average approach creates smoother distribution functions since each marker particle contributes to the average in surrounding cells as well as the one where it is centered.

The cloud temperature is obtained from the conservation of energy principal. As shown in Ermak and Lange[13], the vertically averaged cloud temperature can be calculated from the initial source temperature of the released gas, the ambient temperature, and the location and "energy deficit" associated with each marker particle. The result is

$$T = \left[(\rho - \rho_e) \cdot C_{pa} \cdot T_a + \rho_e \cdot C_{ps} \cdot T_{se} \right] / \left(\rho \cdot C_p \right) \tag{13a}$$

where the effective source temperature is

$$T_{se} = T_a + (T_s - T_a) \cdot \bar{\epsilon} \tag{13b}$$

and the vertically averaged energy deficit is

$$\bar{\epsilon} = (1/N) \cdot \sum_n \omega_n \cdot \epsilon_n . \tag{13c}$$

The time-varying marker particle energy deficit $\epsilon_n(t)$ accounts for the addition of heat to the cloud at the ground surface. This effect is calculated from a rate equation for the marker particle energy deficit that is analogous to the marker particle displacement equations. The rate equation to first order in the time step is[13]

$$\epsilon_n(t+\Delta t) = \epsilon_n(t) / \left[1 + (V_h / h) \cdot \Delta t\right] \tag{14}$$

where V_h is the ground surface energy-transfer velocity defined in Eq. (10) and h is the cloud height. The initial value of $\epsilon_n(o)$ is 1.0 so that the initial effective source temperature is equal to the actual source temperature.

Surface Heating Expansion Displacement. Surface heating of the cloud not only warms the cloud, but also causes it to expand. Calculation of this expansion is straight forward if we assume that the expansion due to surface heating takes place solely in the vertical direction. This assumption is quite realistic especially for cold, dense clouds which are typically much wider than they are high. Using this assumption, the surface heating expansion displacement is found to be[13]

$$\Delta Z_H = \frac{\left(\frac{T_a}{T_o} - 1\right) \cdot \left(\frac{V_h}{h}\right) \cdot Z_o \cdot \Delta t}{\left[1 + (V_h / h) \cdot \Delta t\right]} \tag{15}$$

where $Z_O = Z(t)$ is the height of the marker particle at the beginning of the time step.

The total marker particle displacement in the vertical direction is therefore

$$Z(t+\Delta t) - Z(t) = \Delta Z_H + \Delta Z_D \tag{16}$$

where ΔZ_D is the dispersive displacement due to advection and diffusion given by Eq. (2).

CODE STRUCTURE

All of the dense-gas modifications are included in one of twelve subroutines within the ADPIC code, as shown in Fig. (1). Of the twelve subroutines, five are used to initialize the problem, five are used to calculate the various dense-gas effects including the marker particle energy deficit and trajectories, one is used to set the time step, and one is used to generate the output files. To make these changes, we modified six existing subroutines and added six entirely new subroutines.

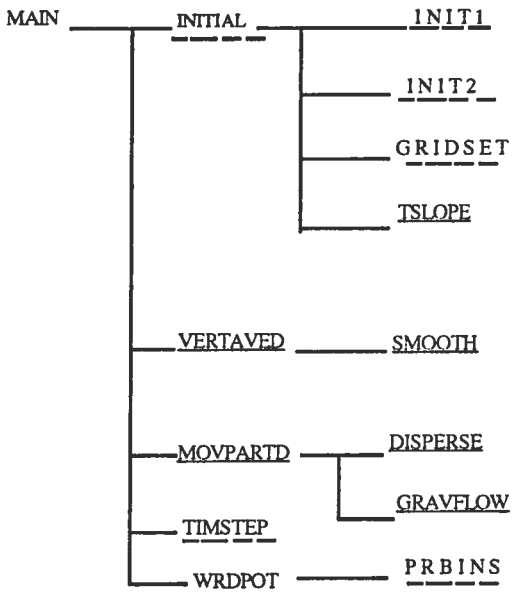

Figure 1. That part of the ADPIC subroutine tree which includes the dense-gas modifications. A dashed underline indicates a pre-existing subroutine that was modified and a solid underline indicates an entirely new subroutine.

All of the dense-gas subroutines are called either directly from the MAIN subroutine or from a subroutine one layer below MAIN. The initialization subroutines are all called from INITIAL and the output subroutine is called from WRDPOT. The initialization and output subroutines perform the following functions.

INITIAL-calls the various initialization subroutines.

INIT1-sets the constants used in the dense-gas algorithms.

INIT2-sets several constants associated with the thermodynamic properties of the atmosphere and checks a number of the input parameters to ensure that they are within realistic limits.

GRIDSET-calculates the physical properties of the dense-gas source including the vertical source velocity.

TSLOPE-calculates the slope of the terrain.

PRBINS-generates the output files of the vertically average cloud properties including: density, temperature, cloud height, mass concentration, mass fraction, and volume fraction.

The Lagrangian particle simulation of the dispersing dense-gas cloud is performed from three subroutines that are called directly from the MAIN subroutine. The subroutine VERTAVED deals with the vertically averaged cloud properties, MOVPARTD deals with the individual marker particle properties and displacement, and TIMSTEP sets the time step to be used in the marker particle displacement and energy deficit equations during the next time cycle. These subroutines perform the following functions and call the following auxiliary subroutines.

VERTAVED-calculates the local cloud height, a surface heating rate parameter, and the vertically averaged cloud properties including: energy deficit, mass concentration, density, temperature, and mass fraction. Calls the SMOOTH subroutine.

-SMOOTH-spatially smoothes the cloud height, surface heating rate parameter, and vertically averaged cloud density, temperature and mass fraction. Calculates the vertically averaged volume fraction from the smoothed mass fraction. (Spatial smoothing is performed to remove spurious gravity waves.)

MOVPARTD-calculates the individual marker particle displacements and energy deficits. Also calculates the advection velocity and diffusivity at the location of each marker particle. To assist in this calculation, MOVPARTD calls the DISPERSE and GRAVFLOW subroutines.

-DISPERSE-calculates the effective friction velocity, entrainment coefficient, and vertical diffusion coefficient at the top of the cloud. Also calculates additional surface heating parameters.

-GRAVFLOW-calculates the three components of the gravity flow velocity.

TIMSTEP-overrides the normal ADPIC time step calculation at the end of each time cycle and sets the time step to the constant value specified in the input data.

VALIDATION CALCULATIONS

We used the dense-gas version of ADPIC to predict the vapor dispersion from two liquefied natural gas (LNG) releases at ground-level onto water. The calculations simulate the vapor dispersion observed in two field-scale experiments, Burro 8 and Burro 9, conducted by the Lawrence Livermore National Laboratory in 1980 at China Lake, California.[14] The composition of LNG is mainly methane which has a molecular weight half that of air. However, LNG is formed by cooling the gas to 112°K so that the source temperature is approximately one-third that of ambient air (~300°K). The net effect is that LNG vapor is about 65% denser than ambient air as well as being much cooler than the ambient air temperature. Consequently, these simulations utilized all of the dense-gas algorithms implemented into ADPIC.

In the Burro 8 and Burro 9 experiments, approximately 25 m^3 of LNG (~6000m^3 of LNG vapor) was released at a nearly constant rate over about one and one-half minutes. Although the release of LNG was onto water (in the form of a small pond), most of the dispersion occurred over land. The source characteristics and meteorological conditions for the two experiments are given in Table 1. The main difference between these two experiments was the meteorological conditions. The Burro 8 test occurred under lower wind speed and more stable ambient atmospheric conditions than did the Burro 9 test.

Table 1. Summary of the Burro 8 and Burro 9 test conditions.

	Burro 8	Burro 9
LNG volume spilled (m^3)	28.4	24.2
Mean LNG spill rate (m^3/min)	16.0	18.4
Mean wind speed at 2 m height (m/s)	1.8	5.7
Mean temperature at 2 m height (°K)	306.	308.
Atmospheric stability class	E	D

The ADPIC simulations were conducted using 5000 marker particles within a $1000 \times 600 \times 28$ m grid. The horizontal grid spacing used in the calculation of the wind field, the three-dimensional concentration distribution, and the vertically average cloud properties was $\Delta x = 25$ m and $\Delta y = 15$ m. The vertical grid spacing used in all of these calculations except the vertically averaged cloud properties (which are independent of the vertical direction) was $\Delta z = 2$ m. And finally, a constant time step of $\Delta t = 2$ s was used throughout the simulations.

A qualitative comparison of the simulated dispersing clouds at comparable times for each of the two tests is given in Fig. (2). In this figure, the dispersing clouds are represented by "dot-plots" where each dot is the location of an individual marker particle projected onto the plane of interest. In Fig. (2a) the cloud is viewed from above looking down onto the horizontal plane and in Fig. (2b) the cloud is viewed from the side with the wind blowing from left to right in both views.

While the gravity flow rates are similar in both simulations (on the order of .5 m/s), the effect on cloud shape is more pronounced in the low wind speed, more stable test of Burro 8. When viewed from above [Fig. (2a)], the simulated Burro 8 cloud is seen to be rounder or "pancake" shaped, while the Burro 9 cloud has the more typical "cigar" shape. In addition, the simulated Burro 8 cloud is wider [Fig. (2a)] and lower [Fig. (2b)] than the Burro 9 cloud. Under the low wind speed conditions of Burro 8, gravity flow has more time to widen the cloud before it travels downwind and dissipates to where the density is essentially equal to the ambient value. Consequently, gravity flow effects on cloud shape are greater in Burro 8 than in the higher wind speed case of Burro 9. Similarly, the dense-gas effect on cloud height is also greater in the simulated Burro 8 test, resulting in a lower cloud in the Burro 8 simulation in comparison to the Burro 9 simulation.

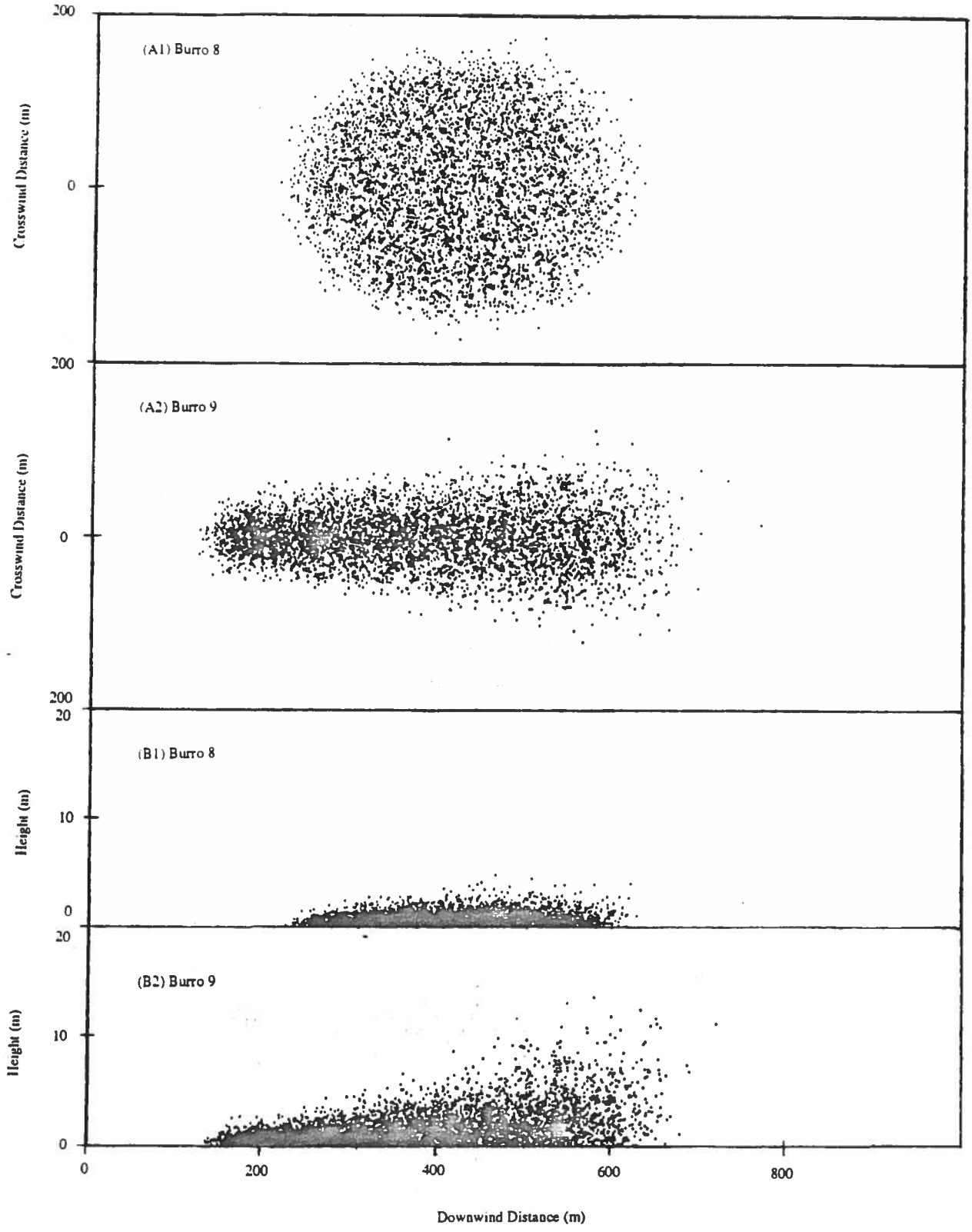

Figure 2. Dot-plot projections of the marker particle locations onto the (A) horizontal and (B) vertical-inwind planes with the wind direction pointing from left to right in both views. Plots (A1) and (B1) are top and side views of the Burro 8 simulation at 4 min. Plots (A2) and (B2) are top and side views of the Burro 9 simulation at 1.5 min.

Table 2. A model-data comparison of peak concentration expressed as the volume fraction.

Burro 8			Burro 9		
Dist. (m)	Calc.	Obs.	Dist. (m)	Calc.	Obs.
57	.63	.58	57	.60	
140	.34	.25+	140	.28	.10
400	.11	.08	400	.074	.035
800	.038	.024	800	.026	.012

These qualitative features of the simulated clouds agree with what was observed in the actual experiments.[14] A more quantitative comparison between the simulated cloud results and experimental observation is given in Table 2 where the peak volume fraction is compared at the four downwind distances where measurements were made. Close to the source, the calculated concentration is in very good agreement with observation. At greater distances from the source, the calculated concentration becomes more conservative (tends to over-estimate concentration) in comparison to observation. At the largest downwind distance, the calculated concentration is about 50% greater than observed in Burro 8 and 100% greater in Burro 9.

In a qualitative comparison of the cloud width and height (not shown), the simulated cloud width was in fair agreement with observation, but the simulated cloud height was somewhat lower than observed. This suggests that the over-estimation of cloud concentration at larger distances may be due to an under-estimation of cloud height in this region.

CONCLUSION

A dense gas version of the ADPIC Lagrangian particle, advection-diffusion model has been developed that is capable of dispersion simulations over terrain with time- and spacially-varying ambient winds. The new dense-gas version includes the physical processes associated with dense-gas dispersion that affect the ambient windfield, turbulent diffusivity, and thermodynamic properties of the dispersing cloud. These effects result in a lower and wider cloud than is observed when a trace or neutral density gas is released and in a cloud that tends to follow the downhill slope of terrain independent of the wind direction. The new dense-gas version of ADPIC is applicable to ground level releases of both ambient-temperature and colder-than-ambient, denser-than-air gases. The dispersion region treated by the model extends from the near-field where dense-gas effects are most pronounced out to the far-field where the originally dense-gas cloud disperses like a trace gas cloud.

During the course of this effort, several numerical and scientific difficulties arose which needed to be resolved in order to create a reliable and robust dense-gas version of the code. Three of the major obstacles were (1) the inability of a fixed grid to resolve the vertical structure and height of low lying dense-gas clouds, (2) the inability of advection-diffusion models to simulate thermal transport, and (3) the occurrence of spurious gravity waves due to the unevenness in the instantaneous marker particle distribution. The vertical resolution problems were solved by using the vertical averaging technique and assumed vertical profiles to calculate the thermodynamic properties of the dense-gas cloud and then using stochastic methods to calculate the dynamics of the marker particle displacements. The inclusion of thermal transport was added to the model by defining a time-varying "thermal energy deficit" property for each marker particle. Then, as the marker particles disperse with time, thermal transport is calculated from the average "thermal energy deficit" within each region of the cloud. And finally, the problem of spurious gravity waves was overcome by using spatial averaging of the gravity forcing functions.

The results of the model simulations conducted to date compare favorably with experimental observation with regard to the centerline concentration, the general cloud shape and the increase in cloud width due to crosswind gravity flow of the dense-gas cloud. The predicted concentration appears to become somewhat conservative (over-predict) with downwind distance (generally within a factor of two) and this result appears to be connected to under-estimating the growth rate of the dense-gas cloud height. Possible causes include over-estimating the damping effect of stable density stratification on the turbulent diffusivity, under-estimating the turbulence

producing effect of surface heating, and over-estimating the gravity flow rate in the higher elevations of the cloud. Since the discrepancies between the model predictions and experiment are within a factor of two, additional comparisons are needed to determine whether the differences are due to systematic deficiencies in the model or the normal variation of the atmosphere.

And finally, a secondary goal of this work, beyond developing a technique for simulating dense-gas dispersion over complex terrain, was to structure these new capabilities in a manner that they could be readily transferred to other codes. Toward this end, a modular approach was used to include the dense-gas modifications within ADPIC, making them easier to transfer to other Lagrangian particle dispersion models. In addition, all of the dense-gas modifications are contained within the ADPIC dispersion code, including those that affect the ambient wind field which is calculated in a separate code. Consequently, the new dense-gas version of ADPIC is not restricted to a single wind flow model; rather, it can be run with alternative wind flow models to provide the ambient wind field. These models include the fully-conservative (mass, momentum, and energy) prognostic wind flow models, as well as the more commonly used data-interpolating, mass-conserving, diagnostic models. This versatility of the dense-gas version of ADPIC allows it to be coupled with a diagnostic wind flow model for emergency response purposes, and then when time constraints are reduced, it can be used with a physically more complete, yet computationally slower, prognostic model.

ACKNOWLEDGMENT

This work was performed for the U.S. Air Force Engineering and Services Center, Tyndall AFB (MIPR N90-29) under the auspices of the U.S. Department of Energy by the Lawrence Livermore National Laboratory under Contract No. W-7405-ENG-48.

REFERENCES

1. Lange, R., "A Three-dimensional Particle-in-Cell Model for the Dispersal of Atmospheric Pollutants and Its Comparison to Regional Tracer Studies," *J. Appl. Meteor.*, **17**, 320 (1978).

2. Lange, R., "A Comparison of the Monte Carlo and the Flux Gradient Method for Atmospheric Diffusion," UCRL-102141, Lawrence Livermore National Laboratory, Livermore, CA (1990).

3. Sullivan, T.J. and S.S. Taylor, "A Computerized Radiological Emergency Response and Assessment System," *Proceedings of an International Symposium on Emergency Planning and Preparedness for Nuclear Facilities*, International Atomic Energy Agency, Rome, Italy, IAEA-SM-280/57.

4. Ermak, D.L. and S.T. Chan, "A Study of Heavy Gas Effects on the Atmospheric Dispersion of Dense Gases," in *Air Pollution Modeling and Its Application*, C. De Wispelaere, F.A. Schiermeier, and N.V. Gillani, Eds., Plenum Press, New York, pp. 723–742 (1986).

5. Koopman, R.P., D.L. Ermak, and S.T. Chan, "A Review of Recent Field Tests and Mathematical Modeling of Atmospheric Dispersion of Large Spills of Denser-Than-Air Gases," *Atmos. Envir.* **23** (4):731 (1989).

6. Ermak, D.L., "User's Manual for SLAB: An Atmospheric Dispersion Model for Denser-Than-Air Releases," UCRL-MA-105607, Lawrence Livermore National Laboratory, Livermore, CA (1990).

7. Ermak, D.L., "A Concept for Treating Dense-Gas Dispersion Under Realistic Conditions of Terrain and Variable Winds," UCRL-JC-104039, Lawrence Livermore National Laboratory, Livermore, CA (1990).

8. Chan, S.T., "FEM3—A Finite Element Model for the Simulation of Gas Transport and Dispersion: User's Manual" UCRL-21043, Lawrence Livermore National Laboratory, Livermore, CA (1988).

9. Ermak, D.L., S.T. Chan, D.L. Morgan, *et al.*, "A Comparison of Dense Gas Dispersion Model Simulations with Burro Series LNG Spill Test Results," *J. Hazardous Materials*, **6**, 129 (1982).

10. Chan, S.T., D.L. Ermak, and L.K. Morris, "FEM3 Model Simulations of Selected Thorney Island Phase I Trials," *J. Hazardous Materials*, **16**, 267 (1987).

11. Hanna, S.R., D.G. Strimaitis, and J.C. Chang, "Uncertainties in Hazardous Gas Model Predictions," *Proceedings of the International Conference and Workshop on Modeling and Mitigating the Consequences of Accidental Releases of Hazardous Materials*, New Orleans, Louisiana, American Institute of Chemical Engineers, pp. 345–368 (1991).

12. Boughton, B.A., J.M. Delaurentis, and W.E. Dunn, "A Stochastic Model of Particle Dispersion in the Atmosphere," *Boundary-Layer Meteor.*, **40**, 147–163 (1987).

13. Ermak, D.L. and R. Lange, "Treatment of Denser-Than-Air Releases in an Advection-Diffusion Model: Thermodynamic Effects," UCRL-JC-106798, Lawrence Livermore National Laboratory, Livermore, CA (1991).

14. Koopman, R.P., R.T. Cederwall, D.L. Ermak, *et al.*, "Analysis of Burro series 40-m^3 LNG spill experiments," *J. Haz. Mat.*, **6**, 43–83 (1982).